Probing Nanodispersions of Clays for Reactive Foaming

G. Harikrishnan,*,† Chris I. Lindsay,‡ M. A. Arunagirinathan,† and Christopher W. Macosko†

Chemical Engineering and Material Science, University of Minnesota, Minneapolis, Minnesota 55455, and Huntsman Polyurethanes, Everberg 3078, Belgium

ABSTRACT Nanodispersions of clays in polyurethane components have been prepared. Nanoclays (both natural and organically modified) of various aspect ratios are used. The fillers are dispersed separately in polyurethane components, viz., polyol and polyisocyanate. The nanodispersions are characterized by the combined use of solution rheology, X-ray scattering, cryo-electron microscopy, and IR spectroscopy. Reactive foaming of these nanodispersions is carried out to make polyurethane nanocomposite foams. The status of the dispersion of fillers in components and in foams has been compared to investigate the effect of the foaming process in exfoliation. Interpretation of the results from different characterization techniques describes the state of the dispersion of fillers in components and in foam. The rheological and physicochemical behaviors of nanodispersions are shown to have a significant influence on the properties of nanocomposite foams.

KEYWORDS: nanodispersion • reactive foaming • polyurethane • barrier property • cell morphology

INTRODUCTION

Reactive foaming, in which the polymerization is conducted simultaneously with foaming, is a versatile technique to produce various types of foams with a wide range of properties. Polyurethane foams are the most common materials made by this technique (1). They find extensive applications as thermal insulation and construction materials, cushioning applications in automobiles/furniture, and electronic packaging. In the formation of polyurethane, hydroxyl and isocyanate functionalities react near room temperature to form urethane linkages. In most cases, a polyfunctional polyol is reacted with an isocyanate. The simultaneous "blowing" or "foaming" of the reacting liquid is accomplished by blowing agents that are added to the polyol component. The foaming could be done by physical blowing, in which low-boiling liquids (such as pentane, hexane, hydrochlorofluorocarbons, etc.) evaporate as a result of the heat of exothermic reactions. Foaming could also be done by chemical blowing in which CO_2, formed by the reaction of water (added to a polyol blend) with isocyanate, causes the expansion. Polyurea is formed as a byproduct during this reaction (2).

Researchers have studied the effect of the addition of nano- and microfillers during reactive polyurethane foaming to enhance the thermal, mechanical, and physical properties of polyurethane foams (3−10). The polymerization and foaming were conducted by dispersion of the fillers, either in polyol or in isocyanate. The oligomer−filler dispersions were reacted with the remaining component, in the presence of catalysts and foaming agents. The results obtained in such studies show mixed trends for various mechanical, physical, and thermal properties of polyurethane foams. Cao et al. reported a substantial increase in the reduced compressive strength (about 600 %) for a semiflexible foam, by dispersion of organically modified montmorillonite (MMT) in an isocyanate component (3). For low-density rigid and flexible foams, when dispersed in a polyol component, various organically modified MMT clays induced powerful cell opening and foam drainage (4). As a result, the compressive strength and thermal resistivity of nanocomposite rigid foams were significantly inferior to those of their conventional counterparts (4). The introduction of hydroxy-tallow-modified MMT to isocyanate is shown to reduce the diffusion of blowing gas out of the foam (5). Mondal and Khakhar found that, for polyurethane foams of high density ($140-160$ kg/m^3), the swelling of rigid foam after immersion in water increased, indicating more open or weak cell windows (6). In this case, the clays were dispersed in polyol. Saha et al. dispersed various nanofillers such as carbon nanofiber (CNF), clay, and nanoparticles of TiO_2 in an isocyanate component and found that CNF gave better enhancement in thermal and mechanical properties compared to clays (7). Javni et al. found that the introduction of micro- and nanosilica particles to rigid and flexible foams decreased the compressive strength of both types of foams (8). Kresta et al. could achieve about 2 % reduction in the thermal conductivity of rigid foams by adding up to 10 % modified MMT (Cloisite 30 B), partly in an isocyanate and the rest in a blowing agent (9).

From the literature, it is clear that the properties of a nanocomposite foam depend on the type of clay used and the component in which it is dispersed. This demands a detailed investigation into the characteristics of component−filler dispersions because the rheological and physico-

chemical behaviors of these blends significantly affect the properties of a foamed polymer. The characterization of a nanofiller−oligomer blend and studies on the nature and quality of such dispersions along with its effect on the processability and properties of a foamed polymer have not been reported yet. The present article also focuses on the barrier effect of various nanoclays to improve the thermal insulation performance of rigid polyurethane foams with aging.

X-ray scattering/diffraction has been conventionally used to identify the crystalline structure of fillers in nanocomposites. It gives a good indication of the dispersed state over a fairly large sample volume. However, it is difficult to interpret the structure and shape of the scattering entity on a reciprocal basis (10). Moreover, because the scattering intensity depends on the concentration of the scattering entity, erroneous interpretations of intercalation/exfoliation could result. Electron microscopy gives a direct visualization of the state of the dispersion of filler. However, it is capable of presenting only a local picture of the status of the dispersion of filler, owing to the limitation of the extremely small sample size analyzed. Rheology has been identified as a useful tool to investigate the dispersion of fillers in nanocomposites and has been employed by many researchers to estimate the filler distribution, both qualitatively and quantitatively (11−17). A polymer melt filled with nanoscale materials is shown to develop a yield stress and a storage modulus that is independent of the frequency (13, 14, 17).

In this study, we have carried out characterizations of dispersions of nanoclays of different chemical nature and aspect ratios with polyurethane components. Reactive foaming of these nanodispersions is carried out to make nanocomposite rigid polyurethane foams. The effect of nanofillers on the morphology, closed-cell content, and barrier properties of a cured foam is also studied. Clays are dispersed separately in polyol and isocyanate. The concentration of the filler in any component is kept constant at 8% by weight of the filler in the oligomer. This particular selection was made in order to make sure that the amount of nanofiller present in the final foamed urethane is 3−6%. The literature on polyurethane foam nanocomposites cited above shows that the optimum filler loading for various property enhancements falls in this particular range. Such a high concentration of the filler will also ensure that the characteristic peaks corresponding to the interlayer spacing of clays are detected by X-rays, even while they are dispersed in components and in foam.

EXPERIMENTAL SECTION

Materials. The polyol selected has an aliphatic polyether backbone (designated hereafter as PEtP) with a functionality of 4.2 and a molecular weight of approximately 800 (Jeffol SD361, Huntsman Polyurethanes). The isocyanate (designated hereafter as MDI) selected was a polymeric methyldiphenyl diisocyanate (Rubinate M, Huntsman Polyurethanes).

Three nanoclays of different aspect ratios and chemical nature were selected. The clays selected were modified laponite (a synthetic smectite, organically modified with a dihydroxytal-

Table 1. Formulation of the Polyol Blend

component	ratio (pbw[a])
polyol Jeffol SD361	100
dimethylcyclohexanamine	2.7
pentamethyldiethylenetriamine	0.3
surfactant Tegostab 8404	2.0
cyclopentane	9.0
water	2.3

[a] Parts by weight.

low) with an aspect ratio of 25−30 (SCPX 3076, Southern Clay), natural montmorillonite (Cloisite Na, Southern Clay) with an aspect ratio of 75−150, and natural vermiculite (Grade 3, Sigma Aldrich) with an aspect ratio of 250−400. The coarse vermiculite obtained was ground in a ball mill and sieved to a maximum size of 38 μm. Hereafter, the clays, viz., modified laponite, natural montmorillonite, and natural vermiculite, are designated by acronyms MLAP, MMT, and VMT, respectively.

Dispersion Technique. All of the clays were dried in a vacuum oven at about 70 °C for 48 h before dispersion in the components. A calculated quantity of clay was added to polyol and isocyanate and was stirred in a closed container for 1 h at moderate speed at a temperature of about 65 °C. This blend was ultrasonicated in a sonicator (L&R Company; frequency = 50−60 Hz, power = 55 W) for 5 h. All of the tests were conducted after at least 24 h of sonication.

Foaming. Foaming agents such as catalysts, surfactant, blowing agents, etc., were added to polyol/polyol−clay blends and stirred at a speed of 2500 rpm for 15 s. The formulation used for the polyol blend is shown in Table 1. A calculated quantity of a MDI/MDI−clay blend was added to the polyol blend and stirred at 2500 rpm for 8 s. The isocyanate index used was 110. The reacting mixture was transferred immediately to a paper-lined rectangular wooden mold of size 32 × 32 × 7 cm³. The mold was then quickly closed, allowing the foam to rise. The foam was demolded after at least 1 h.

Characterizations. *Nanodispersions.* Rheological investigations were carried out by a rheometer (AR G2, TA Instruments) with a parallel-plate assembly. The top plate was 40 mm in diameter. The temperature during measurements was kept constant at 25 °C. The X-ray scattering of dispersions was carried out in transmission mode, by using a microdiffractometer (Bruker AXS). A quartz tube of 2 mm outer diameter (Charles Supper Co.) was used as the sample holder. For crystalline structures of powdered clay samples, an X-ray diffractometer was used (Siemens D5005). FTIR characterization of selected blends was carried out using an IR analyzer (Nicolet Series II Magna-IR System 750) Cryo-scanning electron microscopy (cryo-SEM) of selected dispersions was conducted by using a field-emission cryo-scanning electron microscope (Hitachi S900). The samples were frozen by a high-pressure freezing technique (Balzers HPM 010 high-pressure freezer).

Nanocomposite Foams. The X-ray diffraction of powdered foam samples was conducted by an X-ray diffractometer (Siemens D5005). Transmission electron microscopy (TEM) of nanocomposite foams was done by a transmission electron microscope (JEOL JEM 1210). Samples for TEM were cut using an ultramicrotome (Leica EM UC6). The cell morphology of cured foams was investigated by a scanning electron microscope (JEOL 6500). The closed-cell content was measured as described in ASTM D6226 by a picnometer (AccuPyc 1330, Micrometrics). The thermal conductivity of foams was measured by a steady-state *k*-value analyzer (Fox 150, LaserComp) as described in ASTM C518. Accelerated aging of the foams was conducted to simulate the change in thermal conductivity with time over a period of several years (18). For this, after measurement of the initial thermal conductivity of the samples, the
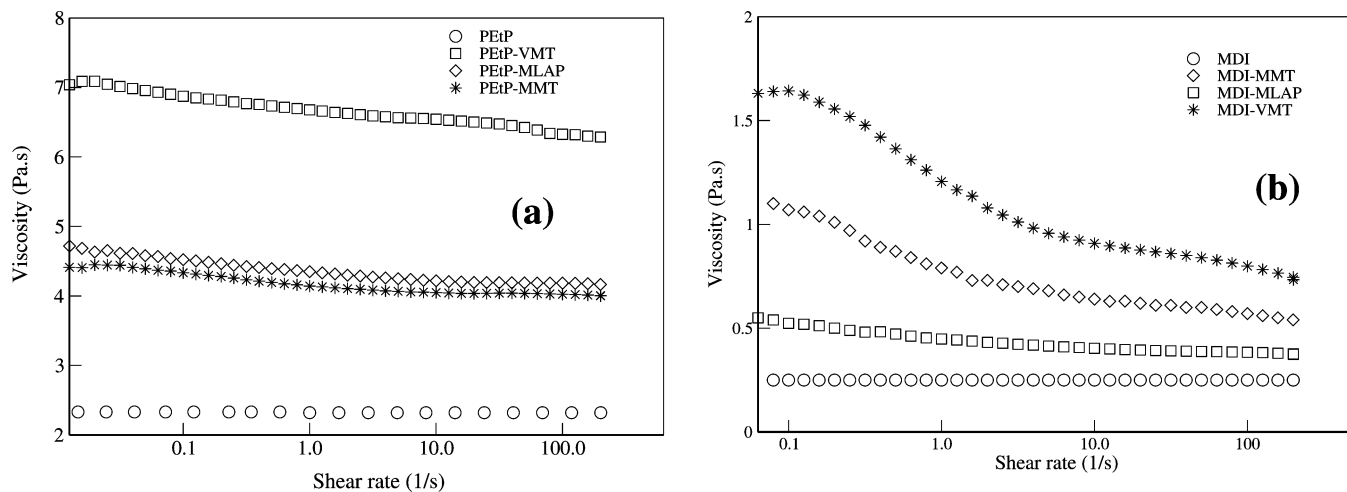
FIGURE 1. Steady-shear viscosities of (a) PEtP−clay blends and (b) MDI−clay blends.

foams were kept in a vacuum oven at 70 °C for 56 days. This accelerates the diffusion of blowing gas out of the foam. The thermal conductivity on the 56th day is estimated. The difference between the initial and final values is found and reported as a percentage change.

RESULTS AND DISCUSSION

Nanodispersions. *Rheology and Processability.* Figure 1 shows the steady-shear and linear viscoelastic behavior of dispersions. It can be seen from Figure 1a that polyol and its dispersions with clays are all Newtonian in behavior. The relative viscosities (η/η_0) of polyol−clay dispersions (compared to neat polyol) are approximately 2.1 (PEtP−MLAP), 1.9 (PEtP−MMT), and 3.0 (PEtP−VMT). The moderate increase in the viscosities for polyol−clay blends is a good indication because the hindrance offered for mixing with an isocyanate component will be low. At the same time, this may also be an indication of a poorly exfoliated state of clays in polyol 4. From Figure 1b, it can be noted that isocyanate has a lower viscosity than polyol and is also Newtonian in behavior. While a MDI−VMT blend shows significant shear thinning, MDI−MMT shows moderate shear thinning. The MDI−MLAP blend is Newtonian and shows a negligible increase in the viscosity. This shows that, while there is a significant interaction of the MDI chains with MMT and VMT, there is phase separation of MLAP in MDI. In both of the above shear-thinning cases, the relative viscosity at high shear rate is approximately 3.0 times, compared to neat MDI. Again, this moderate increase in the high shear viscosity will not hinder blending with the polyol component.

Figure 2 shows the linear viscoelastic behavior of those dispersions that showed shear-thinning behavior during steady-shear experiments. The critical strains during a strain sweep experiment were approximately 1.5% and 1.7% for MDI−VMT and MDI−MMT dispersions, respectively. It can be noted that the storage modulus G' continuously increases and does not become independent, even at high frequencies. This is due to the formation of an incomplete network of platelets of both VMT and MMT in MDI. This shows that, although VMT and MMT have good interaction with MDI, the
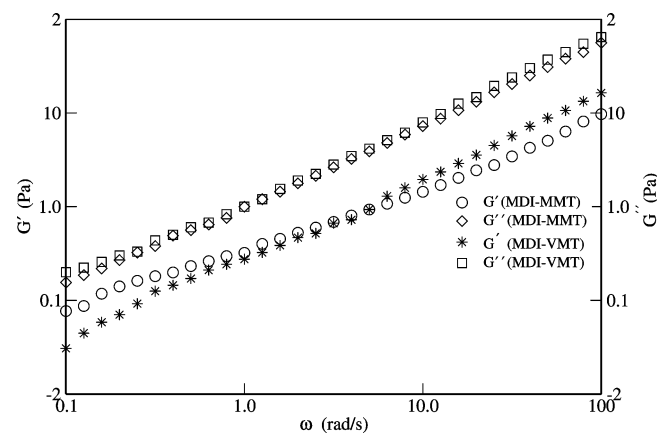

FIGURE 2. Linear viscoelastic behavior of MDI blends with MMT and VMT.

gel structure formed is weak. This indicates the possibility of incomplete exfoliation. As the filler loading exceeds the percolation threshold, a 3D network should develop, resulting in G' remaining constant with the frequency (15, 16).

Structure and Chemistry. The X-ray scattering patterns given in the Supporting Information show the crystalline structure of clays before and after dispersion in components (Figures S1 and S2). It could be inferred that, among all of the clays, the polyol chains could intercalate only into MMT galleries. The disappearance of the characteristic peak of vermiculite, when dispersed in MDI, indicates the possibility of complete exfoliation. In the case of the MMT−MDI blend, there is an indication of the intercalated structure coexisting with partially exfoliated domains as shown by the low-intensity diffused peak. MDI chains did not intercalate into layers of MLAP. These results correlate very well with the steady-shear rheology data. While MDI−VMT and MDI−MMT blends show shear thinning, the blend of MLAP with MDI is Newtonian. However, the complete disappearance of the VMT peak in MDI is not supported by the poor yield stress shown by the blend during linear viscoelastic measurements. Similarly, although the X-ray scattering traces of the MDI−MMT dispersion show considerable intercalation/partial exfoliation, there is no indication of a 3D network formed, as shown by rheology data. To investigate
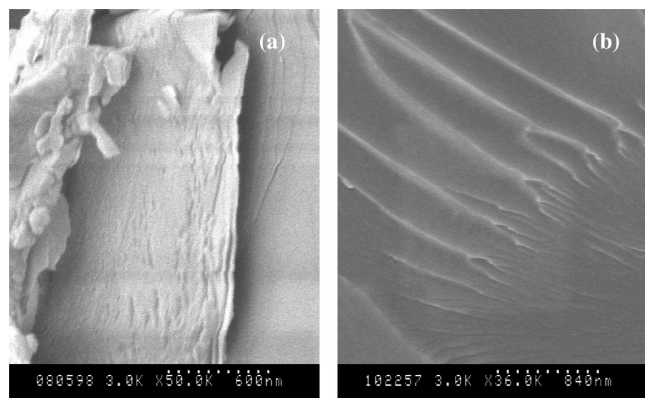
FIGURE 3. Cryo-SEM images of dispersions (a) MDI—VMT and (b) MDI—MMT.

this contradiction, cryo-SEM imaging of these blends was carried out. From the micrograph in Figure 3a, it can be noted that the layered structure of vermiculite is considerably swollen and some single sheets are very well separated from the parent stacked structure. It can also be seen that there are closely layered platelets that are still intact. This shows that vermiculite is only partially exfoliated in MDI with large domains of aggregates present in the dispersion. This is the reason for the formation of a weak gel by this blend. The distance of separation of the layers might be higher than the order of the wavelength of the X-rays so that they undergo undetected during the scattering experiment. Figure 3b shows the images of dispersion of MMT in MDI. In this case, there was no evidence of single layers present in the dispersion. Though the swelling of the clay layers can be seen, there is no indication of exfoliation. It also shows that MMT galleries are much less swollen by MDI, compared to that of vermiculite. This is also manifested by the weak shear-thinning nature of this blend, during rheological measurements.

From FTIR spectra of clays and their blends with MDI (Figure S3 in the Supporting Information), it is seen that —NCO groups reacted with all kinds of hydroxyl moieties on the clay surface. This is clear from the absence of hydroxyl peaks in the case of blends. Reading along with rheological and X-ray scattering data, we see that the reaction of —NCO groups with structural silanol groups facilitates the tethering of MDI chains with clay. The hydroxyl groups of the organic modifier (in the case of MLAP) did not aid in proper chain intercalation.

From the above discussion, it could be inferred that the presence of yield stress during the rheological investigation indicates partial exfoliation of nanoclays. The aspect ratio of clays has no direct relation with the degree of exfoliation. Organic modification of the clay surface was not useful in making a better dispersion. Surface groups of clay that could react with the functional end groups of the components are more effective in tethering oligomer chains with the filler.

Nanocomposite Foams. *Dispersion of Fillers.*
Figure S4 in the Supporting Information shows the X-ray diffraction traces of powdered samples of nanocomposite foams made from nanodispersions. The foaming process did not aid in exfoliation of the clay layers. This is clearly evident
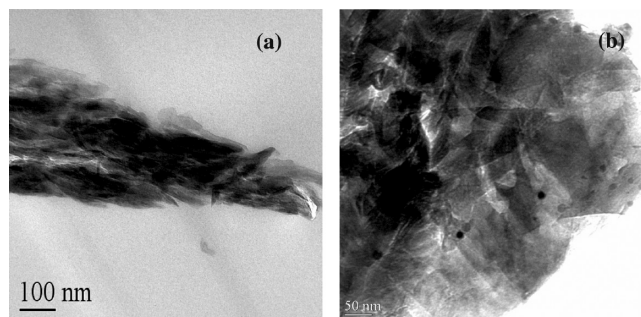

FIGURE 4. TEM images of selected nanocomposite foams: (a) foam made from a MDI—VMT dispersion; (b) foam made from a MDI—MMT dispersion.

from the unchanged peak positions of the clays in nanocomposites, compared to those in dispersions. Thus, it is inferred that no polymerization/bubble nucleation happens inside the clay galleries, irrespective of the types of clays and dispersion media. Figure 4 shows the TEM micrographs of nanocomposite foams made from VMT—MDI and MMT—MDI dispersions. It could be noted that while the dispersion of VMT is much better in PU foams, there are large amounts of aggregates present in the case of foams made from MMT—MDI blends.

Cell Morphology. The cell morphology of neat and nanocomposite foams is shown in Figure 5. From Figure 5c,d, it is observed that the addition of modified laponite to either of the components did not show a significant change in the cell morphology of cured foams. While the addition of MMT to PU components shows a notable cell size reduction, the cell size distribution is not uniform. This is shown by the intermittent presence of big bubbles formed as a result of coalescence (Figure 5e,f). The cell sizes of vermiculite-based nanocomposite foams are much smaller and uniform compared to those of neat foams (Figure 5g,h). It is important to note that while vermiculite dispersed in MDI is in a highly exfoliated state with numerous single sheets of clay present in the dispersion, the polyol—VMT blend shows no reduction in the particle size because there is hardly any exfoliation of VMT in polyol. For smaller cells, the filler should create numerous nucleating sites by reducing the free energy of nucleation (19, 20). Thus, vermiculite is most efficient in creating embryos for nucleation. The fact that vermiculite dispersed in both polyol and isocyanate components could induce small cells of similar size shows that a highly exfoliated state of the filler (length scale of numerous particles at the nanoscale level) does not provide more nucleation sites.

Closed-Cell Content. The closed-cell content of conventional foams and of those made from nanodispersions is found to be $87 \pm 2\%$ and is more or less the same in all cases. Hence, none of the nanofillers induced cell opening/window drainage during foaming. This also indicates that there is no loss of blowing gas out of the foam. Various organically modified MMTs at both exfoliated and intercalated states induced powerful cell opening in PU foams because of the liquid matrix phobicity of the clays (4, 6). Hence, it is inferred that the phenomenon of intercalation/
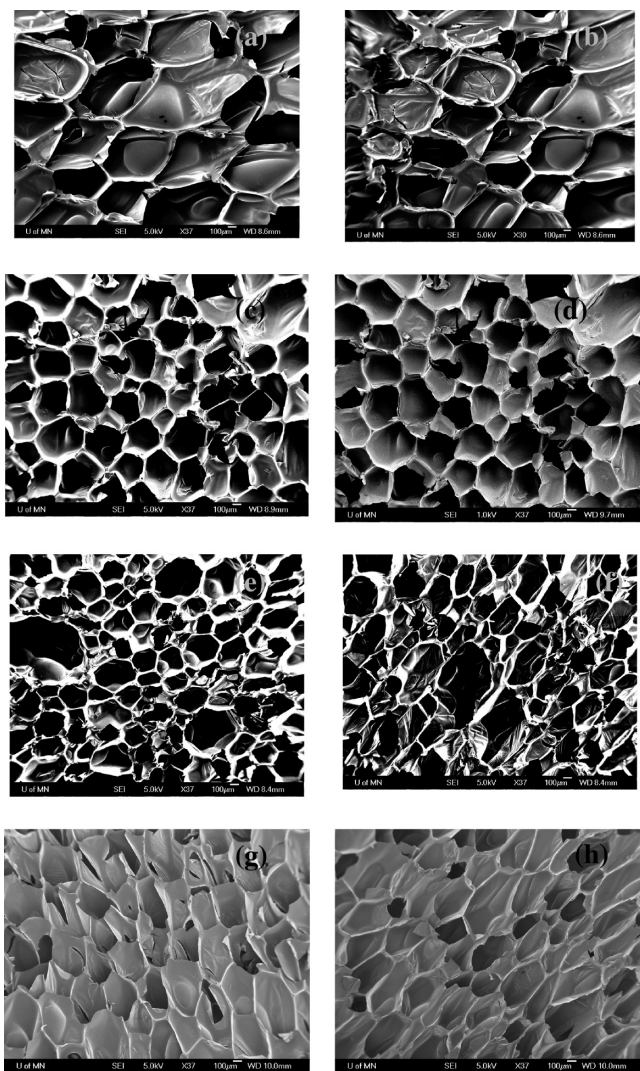
FIGURE 5. SEM micrographs of (a and b) neat PU foams, (c) PU foam from a MDI−MLAP dispersion, (d) PU foam from a PEtP−MLAP dispersion, (e) PU foam from a MDI−MMT dispersion, (f) PU foam from a PEtP−MMT dispersion, (g) PU foam from a MDI−VMT dispersion, and (h) PU foam from a PEtP−VMT dispersion.

exfoliation and, in turn, the difference in the length scales of the filler do not affect foam drainage and cell opening. It is the chemical compatibility of the filler with the reacting liquid matrix that governs the cell opening in nanocomposite PU foams.

Thermal Conductivity and Barrier Effect of Clays. The percentage change in the thermal conductivity of foams after accelerated aging is shown in Figure 6. The percentage change in the thermal conductivity is lowest for foams made from MDI−VMT blends. PU foams made from MDI−MMT and polyol−VMT dispersions register slightly better barrier properties. In all of the other cases, the percentage change is essentially the same as that of conventional foams. This is due to the better dispersion of MDI in isocyanate, providing more surface area and hence a lengthier tortuous path for diffusion of gases (21). It could also be noted that smaller cells induced by heterogeneous nucleation result in a better initial thermal conductivity (22, 23).
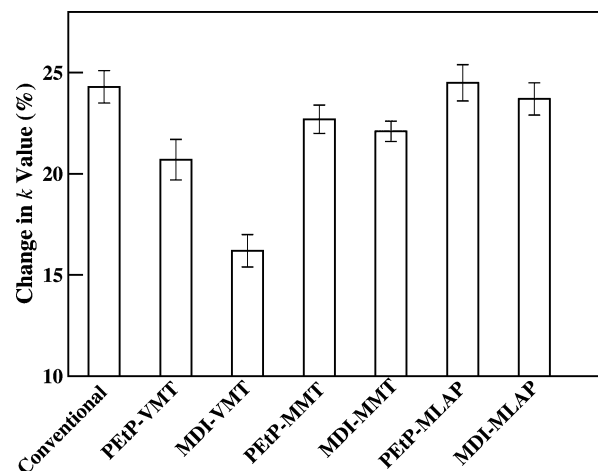

FIGURE 6. Change in the thermal conductivity with accelerated aging of conventional and nanocomposite foams.

Although the direct incorporation of nanofillers to one of the components, followed by polymerization and foaming, provides a useful method for the synthesis of polyurethane nanocomposite foams, the dispersion has to be carefully monitored. The properties of the nanocomposite foam depend on a trade-off between the degree of dispersion/exfoliation of the nanofiller and the increase in the viscosity of the component. The better the degree of dispersion, the higher will be the resulting viscosity of the blend. This will adversely affect the mixing of the components, compromising the quality of the cured foams. On the other hand, small increments in the viscosities of the components by the addition of a nanofiller is an indication of inadequate exfoliation. Careful selection of the component for the dispersion of nanofiller is needed for better properties of the foam.

CONCLUSIONS

Rheological, chemical, and structural investigations of dispersions of various nanoclays in polyurethane components for reactive polyurethane foaming have been conducted. The extent of exfoliation of nanoclays in polyurethane components is shown to have a strong correlation with the rheological behavior of the dispersions. The yield strength of the dispersion gives an indication of the extent of dispersion/aggregation of the nanofiller. Organic modification of the clay did not aid in making a better dispersion. Surface functional groups of clays are shown to be more effective for the tethering of the monomer/oligomer chains to the filler. The selection of the component in which the nanofiller is dispersed could be done using this criterion. No bubble nucleation and growth happens inside the clay galleries, irrespective of intercalation of the components. The properties of foams are significantly influenced by the behavior of dispersions. The status of the dispersion of filler in foam does not affect the cell-opening process. Vermiculite in isocyanate has been shown to be the most effective nanodispersion for making polyurethane nanocomposite foams with better barrier properties. Intercalation/exfoliation of clays in components and in foam did not show a direct correlation with the aspect ratio of the filler.

Supporting Information Available: X-ray scattering/diffraction and FTIR data of clays and dispersions. This material is available free of charge via the Internet at http://pubs.acs.org.

REFERENCES AND NOTES

(1) Randall, D.; Lee, S. In *The Polyurethanes Book,* 2nd ed.; Randall, D., Lee, S., Eds.; Wiley-Interscience: New York, 2002; pp 2−7.

(2) Yasunaga, K.; Neff, R. A.; Zhang, X. D.; Macosko, C. W. *J. Cell. Plast.* **1996**, *32*, 427−448.

(3) Cao, X.; Lee, L. J.; Widya., T.; Macosko, C. W. *Polymer* **2005**, *46*, 775−783.

(4) Harikrishnan, G.; Patro, T. U.; Khakhar, D. V. *Ind. Eng. Chem. Res.* **2006**, *45*, 7126−7134.

(5) Widya, T.; Macosko, C. W. *J. Macromol. Sci., Phys.* **2005**, *44*, 897−908.

(6) Mondal, P.; Khakhar, D. V. *J. Appl. Polym. Sci.* **2007**, *103*, 2802−2809.

(7) Saha, M. C.; Kabir, M. E.; Jeelani, S. *Mater. Sci. Eng., A* **2008**, *479*, 213−222.

(8) Javni, I.; Zhang, W.; Karajkov, V.; Divjakovic, V.; Petrovic, Z. S. *J. Cell. Plast.* **2002**, *38*, 229−239.

(9) Kresta, J. E.; Jinhuang, W.; Crooker, R. M. U.S. Patent 6,518,324, 2003.

(10) Kim, H.; Macosko, C. W. *Macromolecules* **2008**, *41*, 3317−3327.

(11) Krishnamoorti, R.; Gianellis, E. P. *Macromolecules* **1997**, *30*, 4097−4102.

(12) Solomon, M. J.; Almusallam, A.; Seefeldt, S. K. F.; Somwangthanaroj, A.; Varadan, P. *Macromolecules* **2001**, *34*, 1864−1872.

(13) Carastan, D. J.; Demarquette, N. R.; Vermogan, A.; Varlot, K. M. *Rheol. Acta* **2008**, *47*, 521−536.

(14) Madbouly, S. A.; Otaigbe, J. U.; Nanda, A. K.; Wicks, D. *Macromolecules* **2007**, *40*, 4982−4991.

(15) Vermant, J.; Ceccia, S.; Dolgovskij, M. K.; Mafettone, P. L.; Macosko, C. W. *J. Rheol.* **2007**, *51*, 429−450.

(16) Le Meins, J. F.; Moldenaers, P.; Mewis, J. *Ind. Eng. Chem. Res.* **2002**, *41*, 6297−6304.

(17) Jeon, H. S.; Rameshwaram, J. K.; Kim, G. *J. Polym. Sci., Part B: Polym. Phys.* **2004**, *42*, 1000−1009.

(18) Bomberg, M.; Brandreth, D. A. In *Insulation Materials; Testing and Applications,* 1st ed.; McElory, D. L., Kimpflen, J. F., Eds.; ASTM Symposium on Insulation Materials; ASTM: FL, 1987; pp 160−163.

(19) Shen, J.; Zeng, C. C.; Lee, L. J. *Polymer* **2005**, *46*, 5218−5224.

(20) Shen, J.; Han, X.; Lee, L. J. *J. Cell. Plast.* **2006**, *42*, 105−126.

(21) Bharadwaj, R. K. *Macromolecules* **2001**, *34*, 9189−9192.

(22) Theon, J. A. In *Reaction Polymers,* 2nd ed.; Wilson, F. G., Ulrich, H., Riese, W., Eds.; Hanser Publishers: Munich, Germany, 1992; pp 290−292.

(23) Patro, T. U.; Harikrishnan, G.; Misra, A.; Khakhar, D. V. *Polym. Eng. Sci.* **2008**, *48*, 1778−1784.

AM9003123